

INVESTIGATION TO PRODUCTION MOLYBDENUM CONTAINER TO GROWTH SINGLE CRYSTALS BY DEEP DRAWING PROCESS

N. Arab^a, E.A. Nazaryan^b and M. Arakelyan^c

^aIslamic Azad University, Saveh Branch, Iran

^bDepartment of Mechanics, Yerevan State University, Armenia

^cDepartment of Physics, Yerevan State University, Armenia

E-mail: najmarab@iau/saveh.ac.ir

ABSTRACT

A majority of modern electronic and optical devices makes use of the physical properties of single crystals. Such crystals may be organic, inorganic or semimetallic, in nature, and they are usually prepared by synthetic methods. When possible the growth of a material from its own melt is the most convenient way of producing single crystals, two of the most widely used techniques for melt growth being the Bagdasarov, Bridgman-Stockbarger and the Czochralski methods. Common to these and to other methods is a container or crucible to hold the molten material. Clearly a useful crucible material must be chemically compatible with the particular substance to be contained. Molybdenum container is a suitable facility to growth single crystals, because its refractory property and chemical stability, but it is a hardly deformed material which its production require special techniques and technology. In this paper, deep drawing process technology for production boat shape molybdenum container for growing single crystals by horizontal direct growth is discuss. Mechanical properties of sheet molybdenum have been examined and technological features of shaping as well as the temperature regime and strain rate have been researched. Also, optimum conditions to achieve physical kinetics at the crystallization front were considered.

Keywords: Deep drawing, Sheet metal forming, Strain rate, Boat-shaped containers, Single crystal growth.

1. INTRODUCTION

A single crystal, also called monocrystal, is a crystalline solid in which the crystal. Regarding Bagdasarov (2004) and Chen (2005) lattice of the entire sample is continuous and unbroken to the edges of the sample, with no grain boundaries. Grain boundaries have a lot of significant effects on the mechanical, physical and electrical properties of materials. Therefore, single crystals are demanded in many fields, such as microelectronics and optoelectronics, as well as structural and high temperature materials (Schulze, 1981, Giebovsky and Semenov 1995, Nazaryan and Konstantinov 1999). Applications of single crystal materials are broad. Silicon single crystals and related materials have a large market in integrated circuits industry.

Monocrystals of sapphire are highly demanded in laser devices. For metallic materials, turbine blades can be made of single crystals of superalloys, which can achieve novel mechanical properties (Nazaryan and Arab, 2009, Leu, 1999 and Rahul, Verma, and Chandra, 2006). Fortunately, the surface stability of Molybdenum can be combined with its high temperature melting point and chemical durability. The horizontal directed crystallization (the Bagdasarov method 1980) is one of the methods that show promise for growing high-temperature melting single crystals, and its details are illustrated in Fig.1.

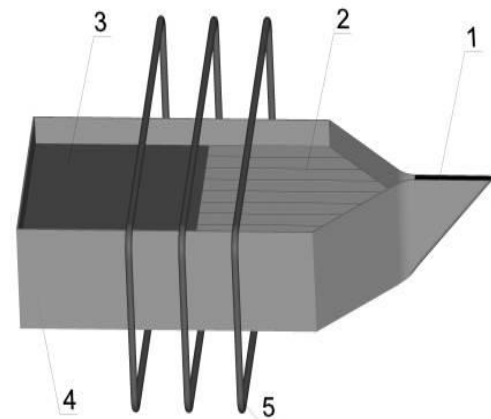


Figure 1. A Schematic of the Bagdasarov Method (1 - Seed, 2 - Crystal, 3 - Melt, 4 - Container, 5 - Heater)

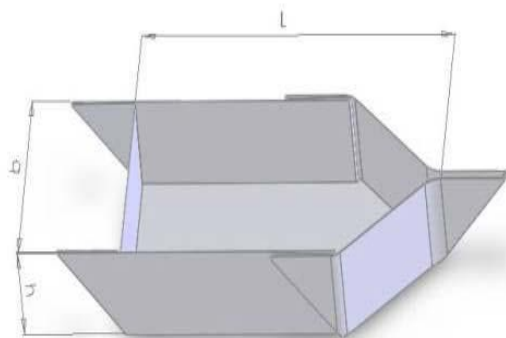


Figure 2. Illustration of Boat Shape Container

The substance to be crystallized is inserted in a boat-shaped container, is molten at dragging of container through the hot zone and then crystallized. The process of growing high-melting single crystals is characterized by temperatures that are critical both by their values and the gradient, respectively 2000°C and 100°C/mm, which stipulate the use of sheet molybdenum for fabrication of containers.

Today, the containers in the form of boat are fabricated from 0.5 mm thick sintered powder sheets of molybdenum by flame hardening process (Fig.2). Both the design and the fabrication technology of containers have a number of inherent drawbacks that impede the formation of required crystallization front and growth of high-quality single crystals (Rohmannudin and Seyrafi, 2009 and US Patent 375096). An analysis of different aspects of horizontal directed crystallization witnesses that the problem of improving the quality and formation efficiency of single crystals is mainly determined by features of container fabrication technology (Abdullah, Bafail, 2007). The boat-shaped containers are thin-wall non-axisymmetric shells which, the main engineering process for its fabrication is the deep drawing. However, the conventional methods of deep drawing proved inapplicable due to low formability of sheet molybdenum.

The aim of the research is to investigate the mechanical properties and processing characteristics of sheet molybdenum under conditions of uniaxial and biaxial stress states and elaboration on their basis of a new technology for deep drawing of containers ensuring optimum conditions to achieve require physical kinetics at the crystallization front (Parasyuk and Romanyuk, 2005 and Chedzey, 1971 and Van Uiter 1970).

2. RELATION BETWEEN STRESSES AND STRAINS IN DEFORMATION OF AXISYMMETRIC THIN-WALL SHELLS

At plastic deformation of axisymmetric thin-wall shell from a sheet metal it is convenient to consider as a reference surface the median plane that halves the material thickness. In this research, rectangular axes are used with z axis in the direction normal to the median surface; ρ extends in radial direction, and θ axis – in the tangential direction perpendicular to both the axes z and ρ . It is taken that the tangential stresses on contacting surfaces of the blank and the tool are small as compared to direct stresses and are negligible, and the radius of curvature in the radial and tangential directions much more exceed the material thickness. By such assumption the principal stresses in the course of deformation coincide with principal axes of strain rates (increments) and the application of zero-moment theory of shells are valid. In the frameworks of assumptions made, the link equations of stresses and strain rates (increments) may be written as:

$$\frac{\sigma_{\rho} - \sigma_z}{\sigma_{\theta} - \sigma_z} = \frac{d\varepsilon_{\rho} - d\varepsilon_z}{d\varepsilon_{\theta} - d\varepsilon_z} \quad (1)$$

where σ_{ρ} , σ_{θ} , σ_z are stresses acting respectively in the radial, tangential and normal-to-median directions, and $d\varepsilon_{\rho}$, $d\varepsilon_{\theta}$, $d\varepsilon_z$ are components of strain increments in the same directions. Under conditions of large plastic strains the metals are practically incompressible and at any stage of deformations the increments of principal strains satisfy the condition of volume stability.

$$d\varepsilon_{\rho} + d\varepsilon_{\theta} + d\varepsilon_z = 0; \quad (2)$$

From Eqs (1) and (2) it follows for the plane stress ($\sigma_z=0$) that:

$$\frac{ds}{s} = \frac{\sigma_{\rho} + \sigma_{\theta}}{\sigma_{\rho} - 2\sigma_{\theta}} \frac{d\rho}{\rho} \quad (3)$$

where, $d\varepsilon_z = ds/s$, $d\varepsilon_{\theta} = d\rho/\rho$, s is the actual thickness of an element of blank, ds is the variation of element thickness with ρ coordinate at its displacement in the center of plastic strain by $d\rho$.

The equation of equilibrium for an element of axisymmetric shell with due regard for the variation of thickness is:

$$\rho \frac{d\sigma_{\rho}}{d\rho} + \sigma_{\rho} \left(1 + \frac{\rho ds}{s d\rho}\right) - \sigma_{\theta} = 0 \quad (4)$$

A combined solution of equations (3) and (4) with the use of plasticity condition for the plane stress:

$$\sigma_{\rho}^2 - \sigma_{\rho} \sigma_{\theta} + \sigma_{\theta}^2 = \sigma_s^2 \quad (5)$$

Gives

$$\rho \frac{d\sigma_{\rho}}{d\rho} + \frac{2\sigma_{\rho}^2}{\sigma_{\rho} - 2\sigma_{\theta}} = 0 \quad (6)$$

In particular cases ($s = \text{constant}$), equation (6) may be integrated and the radial stress may be expressed as an implicit function of coordinate. The efforts to integrate equation (6) with allowance for strain hardening require further simplifying assumptions, the major of which is the constancy of strained material thickness. This assumption is equal to a statement that the plastic deformation of sheet metal proceeds under conditions of plane strain, that, in principle, precludes the

possibility of solving problems, in which a plastic plane stress is the case.

As follows from the condition of volume stability (2), the increments of strain are interdependent and may be depicted in the two-dimensional coordinate system on the plane. As the plane at issue let us consider π -plane of plasticity cylinder, where the state of blank prior to deformation corresponds to the origin of coordinates, and the locus of points, corresponding to successive states of strain represent a strain history. In this case the radial strain histories correspond to proportional variations of principal strains in time. In the general case the current strains are projections of vector-function $\bar{\varepsilon}_i$ on the coordinate axis, and the strain history is described by the vector function $\bar{\varepsilon}_i(p)$ (p is a certain time parameter), the strain rates $d\bar{\varepsilon}_i/dp$ coincide with the tangent to the strain history.

The module of current value $d\varepsilon_i$ is numerically equal to the intensity of strain increments (Chen, 2005).

$$|d\bar{\varepsilon}_i| = d\varepsilon_i = \frac{2}{\sqrt{3}} \sqrt{d\varepsilon_\rho^2 + d\varepsilon_\rho d\varepsilon_\theta + d\varepsilon_\theta^2} \quad (7)$$

The increments of principal strains may be represented in trigonometric form meeting conditions (2) and (7):

$$\begin{aligned} d\varepsilon_\rho &= d\varepsilon_i \cos\varphi & d\varepsilon_\theta &= d\varepsilon_i \cos(\varphi + 2/3 \pi) \\ d\varepsilon_z &= d\varepsilon_i \cos(\varphi + 4/3 \pi) \end{aligned} \quad (8)$$

Where φ is the angle of strain type that may vary within the limits $0 \leq \varphi \leq 2\pi$.

As a result of combined solution of (1), (2) and (8) the dependences of radial and tangential stresses on the angle of strain type are established:

$$\begin{aligned} \bar{\sigma}_\rho &= 2/\sqrt{3} \bar{\sigma}_s \cos(\varphi + \pi/6) \\ \bar{\sigma}_\theta &= -2/\sqrt{3} \bar{\sigma}_s \sin\varphi \end{aligned} \quad (9)$$

which satisfy the plasticity condition (5).

The dependences (10) are circles of $\bar{\sigma}_s/\sqrt{3}$ radius, the centers of which are on lines $\varepsilon_\rho=0$, $\varepsilon_\theta=0$ the circles passing through the origin of coordinates.

The equation of equilibrium (6) may be transformed taking into account dependences (9) and conditions (3), (8), and is written in π -plane in fairly simple form:

$$d\sigma_\rho = \sigma_s d\varepsilon_i \quad (10)$$

Thus, the set of equations characterizing the plastic deformation of axisymmetric thin-walled shells is mapped onto π -plane as a linear dependence between rates of radial stress variation and intensity of deformations. The constant of proportionality in (10) is

the true yield strength of the deformed material, that for convenience may be represented under conditions of cold deformation as a power dependence on the value of accumulated strain:

$$\sigma_s = A\varepsilon_i^n \quad (11)$$

In Fig.3 the relation between stresses (a) and states of strain (b) at axisymmetric shell are shown, that may, in principle, be realized at the plane strain (Nazaryan and Konstantinov, 1999).

To simplify the interpretation of obtained results the origin is matched with axis ε_ρ , and angle φ is taken to increase in counterclockwise direction. At the variation within $0 \leq \varphi \leq 2\pi$ the radial rays divide π -plane into 12 sectors with central angles equal to $\pi/6$. If the strain history coincides with axis ε_ρ , then ε_ρ is the stretching strain (positive), and ε_θ and ε_z are compression strains (negative) that are numerically equal to $\varepsilon_\rho/2$, hence, the strain state is the same as that in the specimen that is subjected to elongation test along ε_ρ axis. One can name this a pure stretching. If the strain history is opposite in direction to axis ε_ρ ($\varphi=\pi$), the strain reverses the sign and corresponds to the pure compression, because in this case ε_θ and ε_z are stretching strains (positive ones) numerically equal to $\varepsilon_\rho/2$. Along strain histories $\varphi=\pi/6$, $\varphi=7\pi/6$ the component of strain $\varepsilon_{z=0}$, and ε_ρ and ε_θ are equal by value and have opposite signs, i.e., here a pure shift or plain stress take place in ρ , θ plane. Analogous reasoning is applicable in cases of strain along ε_θ and ε_z axes, as well as in the opposite and in perpendicular to their directions. So, the strain histories with angles $\varphi=\pi/6$, $\varphi=\pi/2$, $\varphi=5\pi/6$, $\varphi=7\pi/6$, $\varphi=3\pi/6$, $\varphi=11\pi/6$ correspond to pure shift or the plain stress.

The strain histories with angles $\varphi=0$, $\varphi=2\pi/3$, $\varphi=4\pi/3$ correspond to pure stretching, and strain histories with angles $\varphi=\pi/3$, $\varphi=\pi$, $\varphi=5\pi/3$ - to pure compression. At the variation of the angle of strain type within $0 \leq \varphi \leq 2\pi$ the vector-function $\bar{\varepsilon}_i(p)$ alternately is either parallel, or perpendicular to the coordinate axes ε_ρ , ε_θ and ε_z , in consequence of which the components of strain in these axes change from unity to zero.

3. Deep drawing of cylindrical parts

It is easy to show that at deep drawing of a cylindrical part all types of strain are completely characterized by rays covering one third of the coordinate system $5\pi/3 \leq \varphi \leq \pi/3$, show in Fig.3. At deep drawing the edge element of original blank is deformed under conditions of simple compression in the tangential direction ($\varphi=\pi/3$) over all time of deformation process, and ε_ρ and ε_z are stretching strains numerically equal to $\varepsilon_\theta/2$. At the

end of punch, the radial and tangential stresses on the symmetry axis are equal

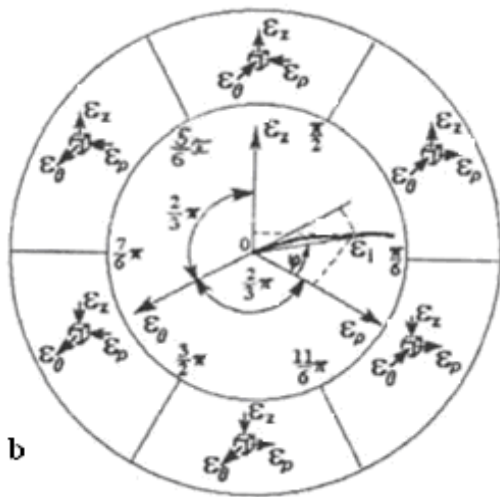
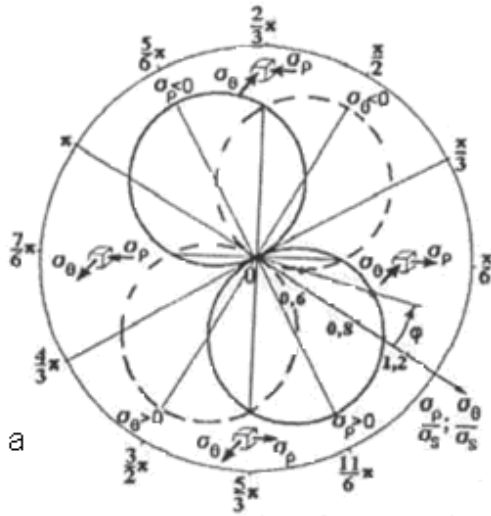


Figure 3. Stress (a) and Strain (b) States of the Axisymmetric Shell (Nazaryan and Konstantinov 1999)

(stretching), and the strain history corresponds to $\varphi = 5\pi/3$ direction. The intervals within $\pi/6 \leq \varphi \leq \pi/3$ and $11\pi/6 \leq \varphi \leq \pi/6$ correspond respectively to increasing and decreasing of the original thickness of blank. There take place two linear compressions, $\varphi = \pi/3$ and $\varphi = 5\pi/3$, in the tangential direction and by thickness, two plane stresses, $\varphi = \pi/6$ and $\varphi = 11\pi/6$, and one linear strain $\varphi = 0$. At the initial stage of drawing process the material is subjected to a biaxial tension in ρ, θ plane, as a result of which a uniform thinning is observed in $\varphi = 5\pi/3$ direction.

In several elements of flange the tensile stresses become equal by value to the tangential compression stress, as a result of which a simple shear or plane stress occurs in ρ, θ ($\varphi = \pi/6$) plane. As the edges of flange shrink, different elements get into the plane stress zone, and because of this the deformation of blank is explicitly not monotone. As the height of element to be drawn increases, the strain histories fill the interval $11\pi/6 \leq \varphi \leq \pi/3$ owing to the presence of punch that prevents shrinkage in tangential direction ($\varepsilon_\theta = 0$). With the help of equations of plastic plane strain on π -plane one can treat the problems of straining the axisymmetric shells at interdependent variation of the thickness and strain hardening without further simplifications. The integration of (10) with due regard for the power dependence of true stress on the value of accumulated strain (11) gives:

$$\sigma_\rho = \frac{A}{n+1} \varepsilon_i^{n+1} + C \quad (12)$$

where the integration constant is obtained from the boundary condition, according to which for the edging element of blank $\varepsilon_i = \varepsilon_{\pi/3}$, $\varphi = \pi/3$ and $\sigma_\rho = 0$ (the edging element is deformed under conditions of linear compression during the whole process of deformation). Equating the expressions for radial stresses from equations (10) and (12) will result:

$$|\varepsilon_i^{n+1} - \varepsilon_{\pi/3}^{n+1}| = (1+n)\varepsilon_i^n \frac{2}{\sqrt{3}} \cos(\varphi + \pi/6) \quad (13)$$

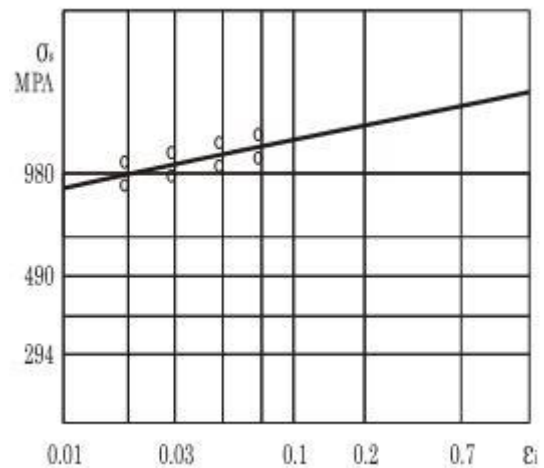


Figure 4. Distributions of Intensity and Strain Components.

The results of above analysis permit a new treatment of the process of flange strain at deep drawing to be made by dividing that into two stages. At the first stage a determined by the equation 14:

$$\frac{R_0}{r_0} = \exp \left[(1 + n) \left(\frac{1}{4} + \frac{\sqrt{3\pi}}{9} \right) \right] \quad (14)$$

formation of the center of plastic strain from the inner boundary to the outer one takes place as the punch is lowered, the elements of blank being stretched in the radial direction. The largest size of plastic zone depends on the parameter of strain hardening and is where R_0 and r_0 are respectively the radii of original blank and the matrix.

In Fig.4 the curves of intensity and variation of strain components are given for the first stage

of strain ($\varepsilon\pi/3$), when the parameter of strain state changes within $0 \leq \varphi \leq \pi/3$ range and $n=0.2$. As follows from these plots, at the initial stage of strain some thickening is formed near the outer contour witnessing to the fact that the punch hold-down pressure is taken by a certain circular zone prior to beginning of flange edge travel.

4. METHODE, RESULTS, AND DISSCUSSION OF EXPERIMENTAL STUDIES

The experiments were conducted with 0.5 mm thick sheet molybdenum of 99.9% chemical purity, with the content of admixtures in fractions of total mass no more than:

% Al – 0.004, %Fe – 0.01, %Ni – 0.005, % Si – 0.01, %C – 0.01, %O₂ – 0.008, % Ca – 0.005.

For determination of dependences of true stresses on actual strains, 50 × 50 × 0.5 mm size specimens were cut from sheet molybdenum for uniaxial tension tests (Leu, 1999).

). The breaking point σ_b and total tensile strain δ have been calculated. The strain rate in all tests was 0.015 m/sec. Based on test results the dependence of σ_s on logarithmic strain $\varepsilon_i = \ln F_0/F$ in logarithmic coordinates, where F_0 and F are the initial and current areas of the cross section respectively. The linear character of the plot allows to approximate the dependence $\sigma_s - \varepsilon_i$ with the power function (Abdullah, Bafail, 2007). (Fig.5).

For sheet molybdenum $A=1080$ MPa; $n=0.048$. The values A and n have been determined graphically as follows: n is the angular coefficient of $\sigma_s = \sigma_s(\varepsilon_i)$ straight line in logarithmic coordinates, A is the value of true stress for $\varepsilon_i=1$, or $A=\sigma_s$ when $\varepsilon_i=1$.

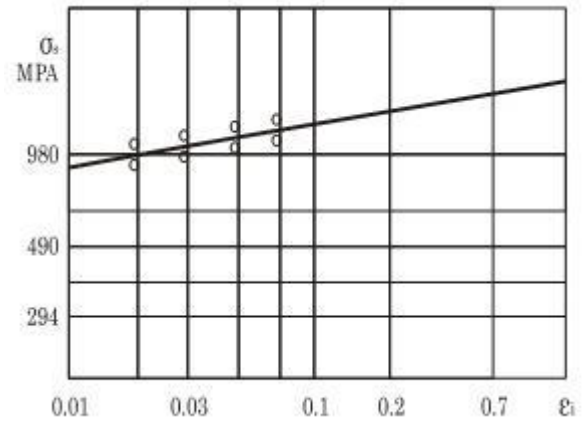


Figure 5. Dependence of σ_s and ε_i in Logarithm Coordinates

The mechanical properties of sheet molybdenum have been calculated by well known relations $\sigma_b = A \cdot n^n \cdot \exp(n)$ and $\delta = \exp(n-1)$, $\sigma_b = 980$ MPa and $\delta = 5\%$. The deep drawing ability of sheet molybdenum was determined by drawing a cylindrical detail, proceeding from the value of limiting drawing ratio $m=d/D$, where D is the largest diameter of blank that was not torn at the test, d is the average diameter of the detail after the drawing. At temperature of 20°C the sheet molybdenum may be both plastic and brittle depending on the content of admixtures and the degree of preliminary strain. Although molybdenum is a refractory metal, its mechanical properties essentially change at comparatively moderate increase of temperature (Bagdasarov, 2004) (Fig.6).

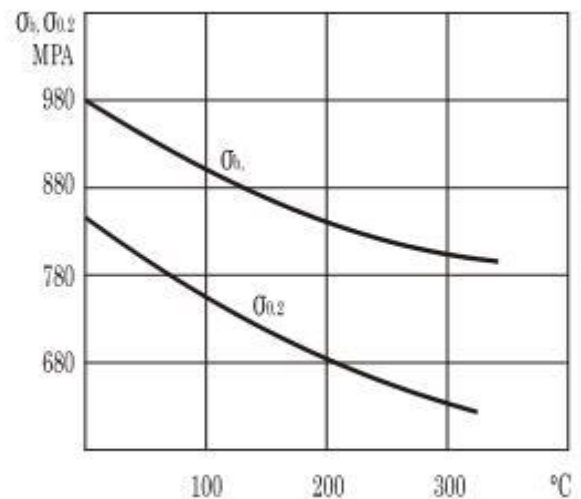


Figure 6. Variation of Mechanical Properties of Molybdenum by Temperature

Since the sheet molybdenum exhibits large heat conductivity and low heat capacity, it is

heated up and cooled off faster than steel, in experiments also the matrix has been heated.

The experiments were performed on a punch with heater and controlled clamp for different strain rates. The clamping force was produced by means of a rubber stopper that was taken out of the heating zone. Forming of corrugation was prevented by regulation of specific clamping force within $4 \div 6$ MPa. The effect of differential heating on the limiting drawing ratio by means of heat transfer from matrix to the peripheral part of flange and cooling of punch has been studied. It was established that the change of deformation degree is achieved owing to the reduction in resistance to flange strain with retention of initial strength at the weak section (Nazaryan and Konstantinov, 1999).

The drawing tests were conducted on general-purpose testing machine having pressing force of 350 kN with controllable strain rate within 0.002 – 0.015 m/sec range. Details of stable high quality were fabricated when $m = 0.6$ and diameter of punch was 40 mm (Fig.7).

The most efficient lubricants for deep drawing of sheet molybdenum with heating to 350°C proved to be aqueous black-lead preparations. These preparations were applied on the heated blank. The lubricant dried up very quickly and the remaining dry thin graphite layer kept on the blank in the course of drawing. The contour of optimum blank for drawing of container has been determined experimentally



Figure 7. Cylindrical Specimens Fabricated by Means of Deep Drawing

by successive approximation method, till articles of similar height around the periphery were obtained and the possibility of overstrain in the weak section was eliminated. The boat-shaped container with $100 \times 215 \times 45$ mm dimension obtained by deep drawing from 0.5 mm thick sheet molybdenum with elongation ratio in the angular sections $m = 0.5$ and radius of 30 mm is shown in Fig.8. The container with a grown single crystal is shown in Fig.9.



Figure 8. The Boat-Shaped Container Fabricated by Means of Deep Drawing.



Figure 9. The Container with Growth Single Crystal.

5. CONCLUSIONS

- 1- Molybdenum container is a new facility to growth single crystals. Making a container from it, require special techniques and technology because it is a refractory metal and hardly deformed material.
2. A novel analytical method for investigation of a stress-state deformation of axisymmetric thin-walled shapes was elaborated, which is base on the analysis of strain histories in π - plane of the plasticity cylinder.
3. The feasibility of theoretical analysis of non-monotonous processes of strain at interdependent variation of thickness and strain hardening was shown.

4. It was established that the strain histories at the deformation of axisymmetric thin-walled shells are in general curvilinear and may stay linear only for edging elements that were not subject to the effect of radial stresses.

5. It was established that the values of strain components that are usually measured during testing of sheet metal at uniaxial and biaxial stresses were π -plane projections of some vector-function (effective strain) and could not serve as characteristics of deep drawing of sheet metal.

6. It was established that for increase in permissible degrees of strain and stabilization of quality of items drawn from sheet molybdenum it is worthwhile to make use of differential heating.

REFERENCES

- Abdullah O. Bafail, Sheikh I. Ishrat, Zahid A. Khan, (2007) " Optimization Of Hydroforming Process For Manufacturing Of Stainless Steel Corrugated Flexible Hose Pipe Using The Taguchi Method", International Journal of Mechanical and Materials Engineering, Vol. 2, No.2, pp.64-70
- Bagdasarov, Kh.S (2004) , "High-temperature rystallization from melt, Moscow, Fizmatlit Publishers,
- Chedzey H. A., et. al, (1971) "A study of the melt growth of single-crystal thiogallates", J. Phys. D: Appl. Phys. 4 pp. 1320-1324 ,
- Chen, H. et. Al. (2005), "Growth of lead molybdate crystals by vertical Bridgman method", Bull. Mater. Sci, Vol. 28, No. 6, Indian Academy of Sciences, pp. 555-560.9
- Crystal Growth Container, US Patent, No. 375096
- Giebovsky, V.G., Semenov, V.N., (1995) Growing Single Crystals of High-Purity Refractory Metals by Electron-Beam Zone Melting", High Temp. Materials and Processes, V. 14, No. 2, pp. 121-130.
- Leu. D. K. (1999) "limiting ratio for plastic instability of the cup-drawing process" Journal of Materials Processing Technology, 86, 168-176.
- Nazaryan, E. A. ,Arab, N. (2009) Deformation at Flanging Circular Holes in Thin Plates , Journal of Blanking Production in Mechanical Engineering , No 3.
- Nazaryan, E.A., Konstantinov, V.F (1999). "Kinematics of straining in deformation operations of sheet stamping" , Moscow, Bulletin of Machine-building, No.2, pp 35 – 41.
- Parasyuk, O.V., Romanyuk, Y.E., and Olekseyuk, I. D., et.al. (2005), J. Alloys Compd., 85, pp 397-403.
- Schulze, K. K. (1981), "Preparation and Characterization of Ultra-High Purity Niobium", JOM, May, , pp 33-44.
- Van Uitert, L.G. (1970) "Platinum Containers for the Growth of Single,Crystal Oxides, Volume 14 Issue 4 , Pages 118-122